B1+ and B1- field pattern dependence on the electrical properties of the sample and the static magnetic field strength

Manushka V. Vaidya[1, 2], Daniel K. Sodickson[1, 2], Ryan Brown[1], Graham C. Wiggins[1], Riccardo Lattanzi[1, 2]
[1]*The Bernard and Irene Schwartz Center for Biomedical Imaging, New York University Langone Medical Center, New York, NY, United States;*
[2]*The Sackler Institute of Graduate Biomedical Sciences, New York University School of Medicine, New York, NY, United States*

INTRODUCTION: The spatial distribution of the B_1 field produced (B_1+) or received (B_1-) by a radiofrequency (RF) coil is affected by the electrical properties of the sample and the strength of the static magnetic field (B_0). This, for example, results in interference patterns near dielectric resonance [1-4], or in the distinctive curling of the B_1- and B_1+ fields observed at high field strengths [5]. While there has been discussion in the literature about interference patterns observed in simulations and experiments versus patterns observed *in vivo* [1-4], intuitive explanations of the behavior of B_1 with respect to electrical conductivity (σ), relative permittivity (ε_r) and Larmor frequency (f_0) are not in wide circulation. A better understanding of unanticipated B_1 field patterns will allow the use of appropriate coils and phantoms. In this study, we show various examples of B_1 field patterns corresponding to different combinations of σ, ε_r and f_0, and provide an explanation for the patterns observed.

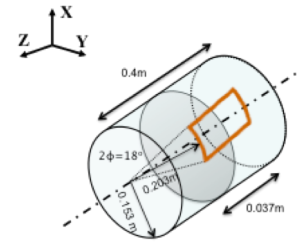

Fig. 1. Object and coil geometry used in the simulations.

THEORY: The asymmetric curling of the B_1+ and B_1- fields inside a dielectric object can be explained by Maxwell's equations. Assuming the magnetic field and electric field are given by $\mathbf{B}(\mathbf{r},t) = \mathbf{B}(\mathbf{r})e^{i\omega t}$ and $\mathbf{E}(\mathbf{r},t) = \mathbf{E}(\mathbf{r})e^{i\omega t}$ respectively, we can write the modified Ampère's law as $\nabla\times\mathbf{B} = \mu_0(\sigma + i\omega\varepsilon_r\varepsilon_0)\mathbf{E}$, where $\omega = 2\pi f_0$. From Faraday's law of induction, $\nabla\times\mathbf{E} = -i\omega\mathbf{B}$, $\mathbf{E}$ is 90° out of phase with $\mathbf{B}$. Therefore, $\mu_0\sigma\mathbf{E}$ in Ampère's law allows the generation of circular polarization, while $\mu_0 i\omega\varepsilon_0\varepsilon_r\mathbf{E}$ is in phase with $\mathbf{B}$ and allows only linear polarization. Thus, the degree of B_1 circular polarization depends principally upon σ and not upon ε_r. The degree of B_1 circular polarization, meanwhile, dictates asymmetries between the spatial distributions of B_1+ and B_1-. Whereas a linearly-polarized B_1 field may be decomposed into equal contributions of right (B_1+) and left (B_1-) circular polarization, a preferentially circularly polarized field will have a larger contribution of one or the other at any given position in the sample. This is the origin of the "curling" of B_1+ and B_1- at high field strength, where asymmetries appear in opposite directions for B_1+ and B_1- fields. Dielectric resonance is a distinct phenomenon in which small stimuli near the natural frequency of the sample result in sustained **E** and **B** field oscillations inside and around the sample [1], which generate standing waves and give rise to a checkerboard-like B_1 field pattern. The B_1 field interference pattern produced by the forward and reflected waves within the sample also depends upon the sample's electrical properties. Consider $k^2=\omega^2\varepsilon_r\varepsilon_0\mu_0(1+i\sigma/\omega\varepsilon_r\varepsilon_0)$, where $k=2\pi/\lambda$ is the complex wave number in the sample. For $\omega\varepsilon_r\varepsilon_0 >> \sigma$, ε_r is inversely proportional to the square of the wavelength (λ^2) in the sample. Additionally, high ε_r concentrates the magnetic flux lines in the sample [6] and reduces energy loss. Therefore, high ε_r is associated with a small λ in the sample and less energy loss, resulting in sustained oscillations of the B_1 field. On the other hand, high σ is associated with a lossy system where the magnetic flux is dispersed [6], resulting in damped oscillations of the B_1 field.

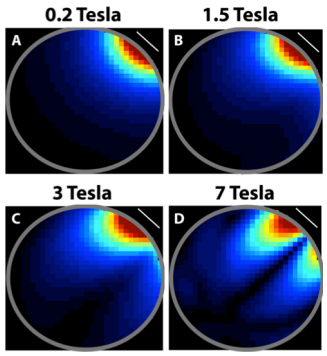

Fig. 2. $|B_1+|$ as a function of B_0 for εr=79 and σ=0.5 S/m, illustrating increased asymmetry at higher field strengths.

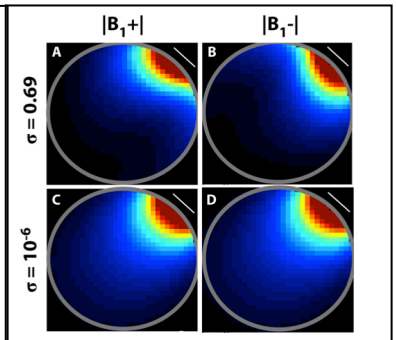

Fig. 3. (B_0=1.5T) $|B_1+|$ and $|B_1-|$ curl in opposite direction when $\sigma > 0$ (A and B), while $|B_1+|$ and $|B_1-|$ are symmetric for a non-conductive sample ($\sigma = 10^{-6}$) with respect to the coil (C and D).

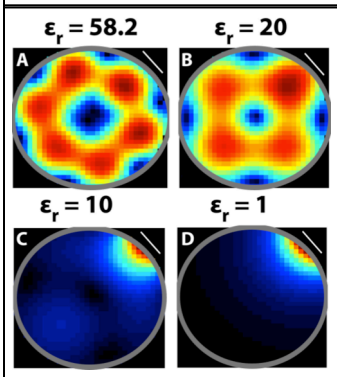

Fig. 4. $|B_1+|$ interference patterns at 7T for a non conductive sample ($\sigma = 10^{-6}$). Field oscillations are reduced with decreasing relative permittivity.

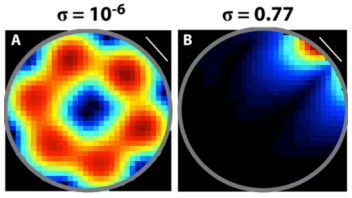

Fig. 5. $|B_1+|$ interference patterns at 7T for ε_r = 58.2 (A). Field oscillations are damped in the conductive sample (B).

METHODS: We used an in-house simulation framework based on dyadic Green's functions to calculate the electromagnetic field in a dielectric cylindrical phantom for a simple rectangular coil [7]. Figure 1 shows the simulation set-up with the dimensions of the phantom and coil. The conductive shield of the MR system was modeled at a distance of 34.25 cm from the axis of the cylinder. All fields were calculated at the proton frequency in the transverse plane at the center of the coil. The following cases were studied as representative examples of the theoretical principles described in the previous section. Figure 2: $|B_1+|$ field pattern as a function of B_0, ranging from 0.2T to 7T, for ε_r=79 and σ=0.5 S/m. Figure 3: The effect of σ on $|B_1+|$ and $|B_1-|$ field patterns at 1.5T. Figure 4 and 5: The effect of ε_r and σ on the $|B_1+|$ interference patterns at 7T.

RESULTS AND DISCUSSION: In each figure, the gray circle marks the boundary of the phantom, and the white line shows the approximate position of the coil. The figures were scaled differently to account for increased magnitude at higher field strengths. As higher field strength implies higher Larmor frequency, the E field in the phantom becomes larger (from Faraday's law), accentuating B_1+ curling in the sample (from the modified Ampère's law) (Fig. 2). Fig 3a and b show opposite curling of B_1+ and B_1-. As expected, there is no field curling or B_1+/B_1- asymmetry when conductivity is removed (Fig 3c,d). Fig 4a shows a strong interference pattern for B_1+ at 7T for a non-conductive sample with ε_r = 58.2. As ε_r is decreased (Fig 4b-d), radiation losses and wavelength of the field increase and at ε_r =1 (Fig 4d), the standing-wave pattern is no longer observed. The interference pattern also vanishes in the presence of conductivity (Fig 5b) due to damped oscillations.

SUMMARY AND CONCLUSIONS: The spatial distribution of the B_1 field in a dielectric cylinder was evaluated for a range of field strengths and sample electrical properties and their effects were explained. While field strength has a predominant effect on the degree of asymmetry between B_1+ and B_1- in the sample, electrical properties play a key role in the magnitude and shape of the interference patterns. Conductivity is responsible for the curling of the B_1 field, and damping field oscillations, thereby preventing standing wave patterns. Relative permittivity reduces energy losses by concentrating the magnetic flux lines and decreases the wavelength of the field, therefore is responsible for large interference patterns observed in samples with very low conductivity values. Note that these ε_r-dependent effects are seldom observed in vivo due to the conductivity of tissues. This conceptual understanding of the factors influencing the B_1 field spatial distribution will be helpful in simulation and phantom experiments where unexpected B_1 field patterns may be observed.

REFERENCES: 1) Collins C., J. MRI 21:192–196 (2005) 2) Moortele P., MRM 54:1503–1518 (2005) 3) Kangarlu A., J. CAT 23(6): 821-831 (1999) 4) Yang Q.X., MRM 47:982–989 (2002) 5) Wiggins GC et al. ISMRM p 393 (2009) 6) Tropp J. ISMRM p 912 (2002) 7) Lattanzi R and Sodickson DK, ISMRM p 3876 (2011)